

**The MACHO Project LMC Variable Star Inventory. VI. The  
Second-overtone Mode of Cepheid Pulsation From First/Second  
Overtone (FO/SO) Beat Cepheids**

C. Alcock<sup>1,2</sup>, R.A. Allsman<sup>3</sup>, D. Alves<sup>1,4</sup>, T.S. Axelrod<sup>5</sup>, A.C. Becker<sup>6</sup>, D.P. Bennett<sup>1,2,7</sup>,  
K.H. Cook<sup>1,2</sup>, K.C. Freeman<sup>5</sup>, K. Griest<sup>2,8</sup>, M.J. Lehner<sup>2,8,9</sup>, S.L. Marshall<sup>1,2</sup>, D. Minniti<sup>1,2</sup>,  
B.A. Peterson<sup>5</sup>, M.R. Pratt<sup>2,6,10</sup>, P.J. Quinn<sup>11</sup>, A.W. Rodgers<sup>5,14</sup>, A. Rorabeck<sup>12</sup>,  
W. Sutherland<sup>13</sup>, A. Tomaney<sup>6</sup>, T. Vandehei<sup>2,8</sup>, D.L. Welch<sup>12</sup>

**(The MACHO Collaboration)**

Received \_\_\_\_\_; accepted \_\_\_\_\_

---

<sup>1</sup>Lawrence Livermore National Laboratory, Livermore, CA 94550 E-mail: [alcock,alves, dminniti, kcook, stuart@igpp.llnl.gov](mailto:alcock,alves, dminniti, kcook, stuart@igpp.llnl.gov)

<sup>2</sup>Center for Particle Astrophysics, University of California, Berkeley, CA 94720

<sup>3</sup>Supercomputing Facility, Australian National University, Canberra, ACT 0200, Australia E-mail: [robyn@macho.anu.edu.au](mailto:robyn@macho.anu.edu.au)

<sup>4</sup>Department of Physics, University of California, Davis, CA 95616

<sup>5</sup>Mt. Stromlo and Siding Spring Observatories, Australian National University, Weston Creek, ACT 2611, Australia E-mail: [tsa, kcf, peterson@mso.anu.edu.au](mailto:tsa, kcf, peterson@mso.anu.edu.au)

<sup>6</sup>Departments of Astronomy and Physics, University of Washington, Seattle, WA 98195 E-mail: [becker, austin@astro.washington.edu](mailto:becker, austin@astro.washington.edu)

<sup>7</sup>Physics Department, University of Notre Dame, Notre Dame, IN 46556 E-mail: [bennett.27@nd.edu](mailto:bennett.27@nd.edu)

<sup>8</sup>Department of Physics, University of California, San Diego, La Jolla, CA 92093 E-mail: [kgriest, tvandehei@ucsd.edu](mailto:kgriest, tvandehei@ucsd.edu)

<sup>9</sup>Department of Physics, University of Sheffield, Sheffield, S3 7RH, U.K. E-mail: [M.Lehner@sheffield.ac.uk](mailto:M.Lehner@sheffield.ac.uk)

<sup>10</sup>LIGO Project, MIT, Room 20B-145, Cambridge, MA 02139 E-mail: [mrp@ligo.mit.edu](mailto:mrp@ligo.mit.edu)

<sup>11</sup>European Southern Observatory, Karl-Schwarzschild Str. 2, D-85748, Garching, Germany E-mail: [pjq@eso.org](mailto:pjq@eso.org)

<sup>12</sup>Dept. of Physics & Astronomy, McMaster University, Hamilton, Ontario, L8S 4M1 Canada E-mail: [welch@physics.mcmaster.ca, rorabeck@glen-net.ca](mailto:welch@physics.mcmaster.ca, rorabeck@glen-net.ca)

<sup>13</sup>Department of Physics, University of Oxford, Oxford OX1 3RH, U.K. E-mail: [w.sutherland@physics.ox.ac.uk](mailto:w.sutherland@physics.ox.ac.uk)

<sup>14</sup>Deceased.

## ABSTRACT

MACHO Project photometry of 45 LMC FO/SO beat Cepheids which pulsate in the first and second overtone (FO and SO, respectively) has been analysed to determine the lightcurve characteristics for the SO mode of Cepheid pulsation. We predict that singly-periodic SO Cepheids will have nearly sinusoidal lightcurves; that we will only be able to discern SO Cepheids from fundamental (F) and (FO) Cepheids for  $P \lesssim 1.4$  days; and that the SO distribution will overlap the short-period edge of the LMC FO Cepheid period-luminosity relation (when both are plotted as a function of photometric period).

We also report the discovery of one SO Cepheid candidate, MACHO\*05:03:39.6–70:04:32, with a photometric period of  $0.775961 \pm 0.000019$  days and an instrumental amplitude of  $0.047 \pm 0.009$  mag in V.

*Subject headings:* Cepheids — Magellanic Clouds — stars: fundamental parameters — stars: oscillations

## 1. Introduction

Gravitational microlensing surveys have produced photometric databases of unprecedented usefulness — both in the number of stars monitored and in the quality and length of their time series. Such databases are favorable hunting grounds for rare (and not-so-rare) types of variable stars and stellar systems.

Among the brightest and most important variable stars are the classical Cepheids. These stars are arguably the most thoroughly understood intrinsic variable from a theoretical standpoint, and are of paramount importance for calibrating the extragalactic distance scale. Microlensing surveys have expanded the number of known Cepheids, which have served to clarify our understanding of Cepheid pulsation. In this paper, we investigate the second-overtone (SO) mode of Cepheid pulsation using LMC first/second overtone (FO/SO) beat Cepheids discovered by the MACHO Project.

## 2. Theoretical Motivation

Stobie (1969a) reported the first theoretical findings suggesting that Cepheids might be unstable in the SO (radial) mode. His non-linear, radiative calculations predicted the existence of SO Cepheids for low  $L$  and high  $T_{\text{eff}}$ , which lead Stobie (1969b) to suggest that such Cepheids might comprise the short-period peak in the SMC Cepheid period distribution. While some early investigations had difficulty in producing SO Cepheids (e.g., Cox 1980 mentioned the SO mode “is frequently not even pulsationally unstable in the linear theory”), most nonlinear calculations (e.g., Chiosi, Wood & Capitano 1993) have confirmed the positive growth rate of the SO mode for Cepheid surface gravities and temperatures, thus predicting that SO Cepheids should exist, provided that real stars could reach the region of instability by normal evolution.

### 3. Observational Motivation

Observational evidence of SO mode excitation in singly-periodic Cepheids has lagged theory by more than two decades. It was only in the 1980s that mode identification of radial pulsators became observationally feasible, guided by predicted period ratios from linear and non-linear calculations: i.e.,  $P_{\text{FO}}/P_F \simeq 0.7$  for the first-overtone (FO) and fundamental (F) modes, and  $P_{\text{SO}}/P_{\text{FO}} \simeq 0.8$ . Two methods are widely used to identify in which modes a Cepheid pulsates: Fourier decomposition of lightcurves, which has become the standard for comparing theory and observation (e.g., Moskalik, Buchler & Marom 1992); and position on the observed P–L relation for extragalactic Cepheids (the F P–L relation or the FO P–L relation, as delimited by Böhm-Vitense 1994 or Alcock et al. 1995).

To date, there exists one possible singly-periodic SO Cepheid candidate: HR 7308, a Galactic Population I Cepheid with constant period (1.491 days), but varying radial velocity (2.3–35 km s<sup>−1</sup>) and V semi-amplitude (0.06–0.17 mag; Andrievsky, Kovtyukh & Usenko 1994). Although HR 7308 is consistent with some SO Cepheid models (Burki et al. 1986; Fabregat, Suso & Reglero 1990; Simon 1985), there are observations which identify it as a FO or F pulsator (Bersier 1996; Bersier & Burki 1996). Thus, it is fair to say that no singly-periodic SO Cepheids have yet been conclusively identified.

Unlike singly-periodic pulsators, beat Cepheids act as calibrators for mode identification: because they pulsate in two modes simultaneously, their period ratios identify their modes of pulsation. Prior to the 1980s, only F/FO beat Cepheids were known to exist. CO Aur, the first (and, so far, only) Galactic FO/SO beat Cepheid, was discovered and analysed by Mantegazza (1983) and Antonello & Mantegazza (1984). However, one star constituted too small a sample for extracting the characteristics of SO Cepheid pulsators. This situation changed when Alcock et al. (1995) provided the first conclusive observational evidence of SO mode excitation by reporting 15 LMC FO/SO beat Cepheids. Alcock et al. also suggested

that singly-periodic SO Cepheids might be found in the MACHO Project LMC database. The motivation for discovering SO Cepheids is straightforward: the common distance of such stars in the LMC, as well as its small amount of differential reddening should allow us to determine unambiguously the  $\log L - \log T_{\text{eff}}$  region where SO excitation occurs.

In subsequent sections we take the first steps towards pursuing this goal, making use of the results of Fourier decomposition of LMC FO/SO beat Cepheid lightcurves to estimate the Fourier parameters of singly-periodic SO pulsators.

#### 4. Fourier Decomposition of Lightcurves: Method

We utilized an expanded sample (compared to Alcock et al. 1995; Welch et al. 1997) of 47 confirmed FO/SO beat Cepheid lightcurves in the LMC discovered by the MACHO Project. Only 45 beat Cepheids are unique: there are two beat Cepheids which were observed in two overlapping MACHO fields.

We refer the reader to Alcock et al. (1995) for a description of our observations and the beat Cepheid identification process. Briefly, each star has two-bandpass photometry (a ‘V’ and ‘R’ band) taken over four years of observation, which results in a time-series for each star of 600–1000 observation epochs. Automatic reduction and analysis routines for these lightcurves provide quality flags for each observation. We used these flags to remove any observations which were suspect because of possible cosmic ray events, bad or missing pixels, or poor image quality. This typically resulted in the rejection of up to 30% of the observations for a given star, since some of these stars are relatively faint.

Each beat Cepheid in our sample can be characterized as pulsating with two non-commensurate frequencies,  $\nu_{\text{FO}}$  and  $\nu_{\text{SO}}$ , and their linear combinations: i.e., any frequencies  $\nu = i\nu_{\text{FO}} + j\nu_{\text{SO}} > 0$ , with  $i$  and  $j$  integer. These frequencies are attributed to FO and SO

interaction within the star. Our goal is to isolate the SO mode of pulsation for each beat Cepheid through Fourier decomposition: i.e., we model a given beat Cepheid’s lightcurve by a truncated Fourier series, examining only the model terms that belong to solely the (FO and) SO modes, ignoring any mixing terms (which typically have much smaller amplitudes than the principle terms). As Pardo & Poretti (1997) pointed out, traditional Fourier analysis involved modeling lightcurves by truncated Fourier series of an *a priori* order, without testing to see which model terms were warranted. To avoid this concern, we opted to code the comprehensive CLEANest algorithm of Foster (1995; 1996a; 1996b) for joint frequency analysis and lightcurve modeling. Foster’s algorithm utilizes an accurate power spectrum estimator (the date-compensated discrete Fourier transform (DCDFT) of Ferraz-Mello 1981) and provides both frequency and model parameter uncertainties. As well, Foster (1996a; 1996b) provides statistical tests of significance for frequencies in a spectrum, and a thorough discussion of how CLEANest differs from other well-known spectral analysis routines.

Our analysis of each beat Cepheid resembles that of Pardo & Poretti (1997). On the first application to a lightcurve, our coding of CLEANest uses the DCDFT of the photometry to produce a power spectrum in the frequency range  $\nu_{\text{res}} = (2T_{\text{span}})^{-1}$  to  $\nu_{\text{max}} = (2\min(\Delta t))^{-1}$  in stepsizes of  $\nu_{\text{res}}$  (the frequency resolution).  $T_{\text{span}}$  is the total time span of the observations for a star, and  $\Delta t$  the minimum time separation between successive observations. If any frequencies in the DCDFT are adopted as significant (the criteria for selection are presented below), each frequency  $\nu_i$  is modeled by  $\cos(2\pi\nu_i t)$  and  $\sin(2\pi\nu_i t)$  terms, plus an overall constant, as prescribed in Foster (1995). The resulting model is subtracted from the original photometry, forming residuals; these residuals are subjected to another DCDFT, and the process is iterated until no significant periodic variations remain in the residuals. Each time a DCDFT of the data or residuals has been performed, CLEANest seeks to find the  $n$ -tuple of frequencies which gives the best description of the

data, by varying each frequency in its neighbourhood until a maximum of Foster (1996a; 1996b)’s model amplitude is found. We allowed CLEANest to perform this frequency variation without requiring that model frequencies retained their expected relations to  $\nu_{\text{FO}}$  and  $\nu_{\text{SO}}$ ; the fact that most model frequencies did retain their expected relation to  $\nu_{\text{FO}}$  and  $\nu_{\text{SO}}$  attested to their authenticity.

What determines whether or not a frequency is significant?  $\nu_{\text{FO}}$  and  $\nu_{\text{SO}}$  were usually found to be the two most powerful frequencies in the first couple DCDFTs of the data<sup>1</sup>, and usually passed Foster (1996a)’s test for statistical significance. Unfortunately, most linear combinations of  $\nu_{\text{FO}}$  and  $\nu_{\text{SO}}$  that we found in DCDFTs failed to pass tests of significance. We thus adopted a frequency as significant if it was a linear combination of  $\nu_{\text{FO}}$  and  $\nu_{\text{SO}}$  (within estimated uncertainties); if it appeared as one of the 20 most powerful frequencies in a residual DCDFT; and if it was reasonable (e.g., we would not have modeled a frequency that seemed to be  $2\nu_{\text{FO}} + \nu_{\text{SO}}$  if we had not previously detected  $2\nu_{\text{FO}}$  or  $\nu_{\text{SO}}$  in our analysis). We terminated our modeling when no frequencies consistent with a linear combination of  $\nu_{\text{FO}}$  and  $\nu_{\text{SO}}$  could be identified in the 20 most powerful frequencies in a residual DCDFT. In most cases, we also had to adopt a model term with a frequency close to  $1.003 \text{ day}^{-1}$ , corresponding to one sidereal day, to make apparent further linear combinations of  $\nu_{\text{FO}}$  and  $\nu_{\text{SO}}$ . In a few cases, we also adopted a model term with one very low frequency, typically around  $0.0005 \text{ day}^{-1}$ , in order to permit further analysis. Scheduling of observations were responsible for the appearance of the sidereal frequency. The small frequency could arise from a zero-point shift in observations, or from a long-period amplitude evolution of the zero-point (mean) of a star, or perhaps from some other cause. Whatever its genesis in a given star, a small frequency has no appreciable effect on our analysis or conclusions, and

---

<sup>1</sup> $\nu_{\text{FO}}$  and  $\nu_{\text{SO}}$  were confirmed by the expectation that  $\nu_{\text{FO}}/\nu_{\text{SO}} \simeq 0.805$  (Alcock et al. 1995).

we do not discuss these further.

In order to test for robustness of CLEANest’s model parameters, we subjected all model parameters in our final CLEANest models to a Marquardt fitting algorithm, a  $\chi^2$  minimization method which pragmatically alternates between a ‘steepest descent’ (or gradient-search) algorithm when  $\chi^2$  changes rapidly near a given set of model parameters, and a first-order model parameter expansion when  $\chi^2$  changes little near a given set of model parameters (e.g., Bevington & Robinson 1992). Most model coefficients and frequencies remained within the uncertainties of their CLEANest values, and retained their relationship to  $\nu_{\text{FO}}$  and  $\nu_{\text{SO}}$  within uncertainties.

In Table 1 we present identifiers, periods, and period ratios for our FO/SO stars. There are two more FO/SO stars than tabulated in Welch et al. (1997). While our results here are not as precise as those listed by Welch et al., they supercede those values. The uncertainties derived in this study are also believed to be better estimates.

Finally, Figure 1 illustrates the results of our fit procedure for a typical FO/SO beat Cepheid. We show lightcurves of the composite, FO, and SO modes of pulsation, along with frequency information. The FO and SO mode lightcurves were derived by prewhitening observations with any model terms not belonging to the displayed mode, as well as mixing terms between modes. The lightcurve shown had the magnitude-average of its observations removed, and is on the instrumental V-band of the MACHO Project.

EDITOR: PLACE FIGURE 1 HERE.

## 5. Fourier Parameters for the SO Mode of Cepheid Pulsation

Our analysis yielded 37 beat Cepheids with robust  $\nu_{\text{FO}}$ ,  $\nu_{\text{SO}}$ ,  $i\nu_{\text{FO}} + \nu_{\text{SO}}$ , and  $i\nu_{\text{FO}}$  frequencies (with  $i$  up to 4), as well as 8 stars with the above plus the  $2\nu_{\text{SO}}$  harmonic. In no case did we detect harmonics higher than  $2\nu_{\text{SO}}$  for the SO mode. We used model coefficients from the FO and SO model terms to form the usual lightcurve geometry indicators:  $R_{k1}$ , the amplitude ratio of the  $(k - 1)$ th harmonic and the ‘base’ frequency model terms for a mode; and  $\phi_{k1} = \phi_k - k\phi_1$ , where  $\phi_k$  is the phase of a mode’s  $(k - 1)$ th harmonic, and  $\phi_1$  the phase of its ‘base’ frequency model term<sup>2</sup>. The absence of any stars with SO harmonics higher than  $2\nu_{\text{SO}}$  clearly limits us to  $R_{21}$  and  $\phi_{21}$  for descriptions of the SO mode’s lightcurve shape, even though up to  $R_{41}$  and  $\phi_{41}$  were possible for the FO mode. We will present these higher-order Fourier decomposition parameters for the FO mode in a future paper.

The Fourier parameters  $R_{21}$  and  $\phi_{21}$  for the FO and SO modes are shown in Figures 2 and 3, plotted against the FO and SO mode periods, respectively: i.e., as their singly-periodic counterparts would appear in such plots. All stars appear in the FO sequences.

Only a small fraction of our beat Cepheids clearly exhibited  $2\nu_{\text{SO}}$ , needed to form  $R_{21}$  and  $\phi_{21}$ . In order to try and draw out as much information on the SO mode as possible, we adopted a  $2\nu_{\text{SO}}$  from the best-fit  $\nu_{\text{SO}}$  for each of the 37 stars which did not exhibit a  $2\nu_{\text{SO}}$  variation using CLEANest, and attempted to fit model terms for such a frequency with our Marquardt algorithm, keeping only those stars whose best-fit result was consistent with our initial guess. Eighteen extra stars had such ‘stable’  $2\nu_{\text{SO}}$  frequencies. We added

---

<sup>2</sup>Original use of  $R_{k1}$  and  $\phi_{k1}$  is commonly attributed to Simon & Lee (1981), but related quantities were used and defined in e.g., Payne-Gaposchkin (1947) and Kukarkin & Parenago (1937). Note that  $\phi_{k1}$  is independent of reference epoch.

them to Figures 2 and 3, broadening our SO mode sequences to a greater range of periods ( $0.49 < P < 1.1$  days). The remaining 19 stars failed to have a stable  $2\nu_{\text{SO}}$  and so have a SO mode with a purely sinusoidal lightcurve shape: i.e.,  $R_{21} = 0$ . These 19 stars are shown in Figure 2, but not in Figure 3, as their  $\phi_{21}$  values are undefined.

EDITOR: PLACE FIGURE 2 HERE.

EDITOR: PLACE FIGURE 3 HERE.

## 6. Discussion

### 6.1. The Long-Period Limit for Identification of LMC SO Cepheids

Recent theoretical investigations examining the SO mode of Cepheid pulsation suggest that SO Cepheids can have periods of 10 days or more (e.g., the comprehensive study of Chiosi et al. 1996). We are in the position to add some observational constraints on this long-period limit.

Figure 4 shows  $R_{21}$  and  $\phi_{21}$  for all known LMC singly-periodic Cepheids with  $R_{21}$  uncertainties less than 0.05 and  $\phi_{21}$  uncertainties less than 0.1 rad, discovered by the MACHO Project (adapted from Welch et al. 1997). Over 1400 Cepheids are displayed, but all avoid combinations of  $R_{21}$  and  $\phi_{21}$  in regions we expect for a SO pulsator (the hatched regions in the Figure, derived from our Figures 2 and 3). If Figure 4’s sample of Cepheids is indicative of LMC Cepheids as a whole over their period range, we would expect to see at least some stars in the longer-period SO sequence range — say around 1 day — but we do not see any. This is true even when restrictions on  $R_{21}$ ’s and  $\phi_{21}$ ’s uncertainties are removed: no SO candidates appear in the shaded region of the  $R_{21}$ –P portion of the Figure.

Those stars which lie in the shaded region of the  $\phi_{21}$ –P portion of Figure 4 have  $R_{21}$  values consistent with FO and F pulsators.

EDITOR: PLACE FIGURE 4 HERE.

The lack of  $P \lesssim 1$  day Cepheid candidates may be the result of a bias — in that Figure 4’s Cepheids were selected for periods of about 1 day or longer, as well as CMD position, P–L position, and lightcurve shape. However, the lack of an obvious third Fourier parameter sequence at periods longer than 1 day is probably real, as one would surmise from the greater density of stars in Figure 4 to longer periods. This suggests that SO Cepheids are indeed a rare species.

It would be intriguing if the  $R_{21}$  SO sequence mimicked the ‘V’ shape of the FO and F mode  $R_{21}$  sequences of Figure 4. What we see in Figure 2 would be the short-period commencement of such a sequence, and we would expect, analogous to the sequences in Figure 4, a drop to zero followed by a sharp rise in  $R_{21}$  on the long-period side of this drop. Such behaviour has been predicted for SO Cepheids, attributed to a resonance between the second and sixth overtone modes around SO periods of 1 day (Antonello & Kanbur 1997). Presumably, the rising branch of  $R_{21}$  for the SO mode would be hidden in the FO sequence we see in Figure 4. This would limit our ability to discern SO Cepheids based on lightcurve shape to stars with periods less than about 1.4 days.

## 6.2. Lightcurve Shape: Observations vs. Theoretical Suggestions

The first investigation of lightcurve shape for SO radial pulsators by Stellingwerf, Gautschy & Dickens (1987) suggested such stars would have the characteristic ‘sawtooth’ nature of F lightcurves, based on Fourier decompositions of one-zone models. While this suggestion was used to identify SO RR Lyrae stars (the ‘RRe’ stars of Alcock et al. 1996),

the Fourier parameters of Figures 2 and 3 do not comply with such a suggestion for SO Cepheids, which would require  $R_{21} \gtrsim 0.3$  and  $\phi_{21} \simeq 4.0$  rad. This non-conformity is not unexpected: as our referee noted, one-zone models of RR Lyrae-type pulsations may not have much bearing on actual lightcurves of SO Cepheids. Antonello & Kanbur (1997) have recently completed a SO Cepheid pulsation study which indicates lightcurves of a type “more sinusoidal than [FO] ones, at least for short periods” (about 1 day or less). Observationally, we find sinusoidal — or nearly sinusoidal — lightcurves to be the norm for the Cepheid SO mode. Pardo & Poretti (1997) suggested as much for CO Aur, the sole Galactic FO/SO beat Cepheid, when they failed to detect its  $2\nu_{\text{SO}}$  frequency. Future observational and theoretical investigations should be guided by this finding: that SO Cepheids have a symmetric, nearly-sinusoidal light variation over their pulsational cycle.

This has a bearing on nomenclature. Some authors use the term ‘s–Cepheid’ (e.g., Antonello, Poretti, & Reduzzi 1990; Morgan 1995) for stars that are, largely, FO Cepheids (as shown most recently for Galactic Cepheids by Pardo & Poretti 1997). We have shown that SO Cepheids are distinctly more sinusoidal in lightcurve shape than FO and F Cepheids from their low  $R_{21}$  values. It might be better to refer to s–Cepheids instead as first overtone (FO) Cepheids in the future, to avoid ambiguities.

## 7. A LMC SO Cepheid Candidate

During the extraction and inspection of variables from a section of the CMD for our four years of LMC observation, we discovered MACHO\*05:03:39.6–70:04:32, a small-amplitude sinusoidal pulsator. In Figures 5 and 6 we show its position in the P–L relation and CMD for known LMC Cepheids. Although it occupies sparsely populated regions in these diagrams, it is, most probably, a classical Cepheid.

EDITOR: PLACE FIGURE 5 HERE.

EDITOR: PLACE FIGURE 6 HERE.

We transformed this star’s MACHO V- and R-band photometry to V and  $R_{KC}$  using our latest transformation equations, and subjected its observations to the fitting procedure outlined above. The results for the V band are displayed as Figure 7. We found all bandpasses were best described by a single component,

$$X(t) = X_0 + \Delta_X \cos(2\pi(t - t_0)\nu_X + \phi_X),$$

where  $X$  is one of V or  $R_{KC}$ , and  $t_0 = \text{JD } 2448628.632$ . The coefficients from these fits are presented in Table 2. A frequency corresponding to  $1.003 \text{ days}^{-1}$  was also adopted in both fits, but made no difference to their appearance. MACHO\*05:03:39.6–70:04:32 stands as a (serendipitous) first extragalactic SO Cepheid candidate.

EDITOR: PLACE FIGURE 7 HERE.

## 8. Future Directions

We are, at present, actively searching for more singly-periodic SO Cepheids in the MACHO LMC and SMC databases. Any additional SO candidates will be reported in a future paper.

The number of short-period pulsators will increase as one moves to lower metallicity environments (e.g., Lipunova 1992). Thus, the SMC should provide an even better hunting ground for beat Cepheids and SO candidates when the MACHO Project analysis of SMC photometry is complete.

We are grateful for the skilled support given our project by the technical staff at Mt. Stromlo Observatory (MSO). Work performed at Lawrence Livermore National Laboratory (LLNL) is supported by the Department of Energy (DOE) under contract W7405-ENG-48. Work performed by the Center for Particle Astrophysics (CfPA) on the University of California campuses is supported in part by the Office of Science and Technology Centers of the National Science Foundation (NSF) under cooperative agreement AST-8809616. Work performed at MSO is supported by the Bilateral Science and Technology Program of the Australian Department of Industry, Technology and Regional Development. KG acknowledges a DOE OJI grant, and the support of the Sloan Foundation. DLW and AJR were supported, in part, by a Research Grant from the Natural Sciences and Engineering Research Council of Canada (NSERC) during this work. AJR was also supported, in part, by an NSERC Postgraduate scholarship (PGS A). This work comprised part of his M.Sc. thesis.

## REFERENCES

Alcock, C. et al. 1995, AJ, 109, 1653

Alcock, C. et al. 1996, AJ, 111, 1146

Andrievsky, S. M., Kovtyukh, V. V., & Usenko, I. A. 1994 A&A, 281, 465

Antonello, E. & Mantegazza, L. 1984, A&A, 133, 52

Antonello, E., Poretti, E., & Reduzzi, L. 1990, A&A, 246, 341

Antonello, E. & Kanbur, S. M. 1997, MNRAS, 286, L33

Bersier, D. & Burki, G. 1996, A&A, 306, 417

Bersier, D. 1996, A&A, 308, 514

Bevington, P. R., & Robinson, D. K. 1992, Data Reduction and Error Analysis for the Physical Sciences (New York: Mc-Graw Hill)

Böhm-Vitense, E. 1994, AJ, 107, 673

Buchler, J. R. & Moskalik, P. 1994, A&A, 292, 450

Buchler, J. R., Kolláth, Z., Beaulieu, J. P., & Goupil, M. J. 1996, ApJ, 462, L83

Burki, G. et al. 1986, A&A, 168, 139

Carpino, M., Milani, A., & Nobili, A. M. 1987, A&A, 181, 182

Chiosi, C., Wood, P. R., & Capitano, N. 1993, ApJS, 86, 541

Christensen-Dalsgaard, J., & Petersen, J. O. 1995, A&A, 308, L661

Cox, A. N. 1980, ARA&A, 18, 15

Fabregat, J., Suso, J., & Reglero, V. 1990, MNRAS, 245, 542

Ferraz-Mello, S. 1981, AJ, 86, 619

Foster, G. 1995, AJ, 109, 1889

Foster, G. 1996, AJ, 111, 541 (1996a)

Foster, G. 1996, AJ, 111, 555 (1996b)

Kukarkin, B. W., & Parenago, P. P. 1937, Astr. J. Soviet Union, 14, 186

Lipunova, N. A. 1992, in Variable Star Research: An International Perspective, ed. J. R. Percy, J. A. Mattei & C. Sterken (Cambridge: Cambridge Univ. Press), 55

Mantegazza, L. 1983, A&A, 118, 321

Morgan, S. 1995, AJ, 109, 1263

Morgan, S. & Welch, D. L. 1997, AJ, 114, 1183

Moskalik, P., Buchler, J. R. & Marom, A. 1992, ApJ, 385, 685

Pardo, I. & Poretti, E. 1997, A&A, 324, 121

Payne-Gaposchkin, C. 1947, AJ, 52, 218

Poretti, E. & Pardo, I. 1997, A&A, 324, 133

Simon, N. R. 1979, A&A, 74, 30

Simon, N. R. & Lee, A. S. 1981, ApJ, 248, 291

Simon, N. R. 1985, in Proc. IAU Coll. 82, Cepheids: Theory and Observations, ed. B. Madore (Cambridge: Cambridge University Press), 93

Simon, N. R. 1990, in ASP Conference Series, Vol. 11, Confrontation Between Stellar Pulsation and Evolution, ed. C. Cacciari & G. Clementini (San Francisco: ASP), 193

Stellingwerf, R. F., & Donohoe, M. 1986, ApJ, 306, 183

Stellingwerf R. F., Gautschy, A., & Dickens, R. J. 1987, ApJ, 313, L75

Stobie, R. S. 1969, MNRAS, 144, 461 (1969a)

Stobie, R. S. 1969, MNRAS, 144, 511 (1969b)

Vaníček, P. 1971, Ap&SS, 12, 10

Welch, D. L. et al. 1997, Proceedings of the Twelfth IAP Colloquium on Variable Stars and the Astrophysical Returns of Microlensing Surveys, eds. R. Ferlet, J. P. Maillard & B. Raban, Editions Frontières, p.205

Fig. 1.— Model results for a typical beat Cepheid. The top left panel displays the lightcurve phased with the FO mode period, 0.715871(18) days. The middle left panel displays the best-fit FO mode solution, while the bottom left panel displays the best-fit SO mode solution. The error bar on the left-hand plots is typical. The topmost right panel displays the amplitude spectrum (DCDFT) of the original photometry — a series of significant frequencies and their aliases. The middle right panel displays the amplitude spectrum for the DCDFT of the final residuals, superimposed with the best-fit  $n$ -tuple of frequencies for the star. The bottom right panel shows the residual spectrum of the middle right panel on a finer scale, with the best-fit  $n$ -tuple frequencies removed. No significant frequencies are apparent.

Fig. 2.— The amplitude ratio  $R_{21}$  for the FO and SO modes of our beat Cepheids, using all stars with stable  $2\nu_{\text{SO}}$  frequencies, whether they were detected using the CLEANest algorithm (8 filled triangles) or introduced after using CLEANest, but found to be stable (18 open triangles). The remaining stars with  $R_{21} = 0$  are also shown.

Fig. 3.— The Fourier phase  $\phi_{21}$  for the FO and SO modes of our beat Cepheids, using the same stars and symbols as Figure 2. Stars with  $R_{21} = 0$  have undefined phases, and so do not appear in the plot.

Fig. 4.— The Fourier parameters  $R_{21}$  and  $\phi_{21}$  for MACHO Project Cepheids in the LMC, adapted from Welch et al. (1997). The sequences in  $R_{21}$  and  $\phi_{21}$  extending to the longest periods are the F mode sequences; the other sequences belong to the FO mode. The hatched region delimits SO mode boundaries as found in Figures 2 and 3 for SO mode Cepheids with  $R_{21} \neq 0$ . Any stars with  $\phi_{21}$  in the hatched region have  $R_{21}$  values indicative of F and FO pulsators.

Fig. 5.— The P–L relation for MACHO Project LMC Cepheids shown in Figure 4, along with MACHO\*05:03:39.6–70:04:32, our SO candidate (the filled triangle).

Fig. 6.— The CMD for MACHO Project LMC Cepheids from Figure 4, along with MACHO\*05:03:39.6–70:04:32, our SO candidate (the filled triangle).

Fig. 7.— Our photometry and model fit for MACHO\*05:03:39.6–70:04:32 in the V band. The left panels show the actual data and the model fit, phased with a period of 0.775961(19) days. The lower panel does not include the sidereal day model term, but shows no appreciable difference from the top panel. The right panels show the DCDFT of the raw data (top), the final residual DCDFT plus the best-fit frequencies ( $\nu_{SO}$  and a sidereal frequency; middle), and the residual DCDFT (bottom).

Table 1. LMC FO/SO Beat Cepheid Periods and Period Ratios

Cepheid <sup>a</sup>	ID <sup>b</sup>	$P_{\text{FO}}$ (days)	$P_{\text{SO}}$ (days)	$P_{\text{SO}}/P_{\text{FO}}$
MACHO*05:11:39.9–68:49:58	79..5022..339	0.526264(09)	0.422854(12)	0.803502(26)
MACHO*04:53:15.5–68:16:37	47..2127..102	0.578469(20)	0.466607(35)	0.806623(67)
MACHO*05:38:51.1–69:49:24	81..9485...45	0.610981(13)	0.491236(16)	0.804012(31)
MACHO*05:48:55.2–70:30:03	12.11168..150	0.640684(13)	0.516399(11)	0.806012(24)
MACHO*05:15:35.2–68:57:08	79..5747..197	0.665188(20)	0.536387(11)	0.806369(30)
MACHO*05:15:05.4–69:39:55	5..5615.2564	0.689983(15)	0.555710(12)	0.805398(25)
MACHO*05:15:06.3–69:39:54	78..5615...82	0.689986(16)	0.555687(15)	0.805360(29)
MACHO*05:35:11.1–70:17:06	11..8873..189	0.704752(16)	0.568415(13)	0.806547(26)
MACHO*05:16:28.6–69:36:34	78..5858..301	0.711555(16)	0.574158(13)	0.806906(26)
MACHO*05:24:13.9–68:49:35	80..7080.2618	0.715871(18)	0.577964(14)	0.807358(28)
MACHO*05:30:01.9–69:11:39	82..8042..142	0.724083(18)	0.584623(15)	0.807399(29)
MACHO*05:26:02.1–69:52:10	77..7427..306	0.729248(17)	0.588430(14)	0.806900(27)
MACHO*05:37:47.1–70:51:44	11..9348...78	0.737788(18)	0.594408(14)	0.805662(27)
MACHO*05:26:01.5–69:30:42	77..7432..248	0.740806(18)	0.595110(14)	0.803327(28)
MACHO*04:58:53.0–68:51:08	18..2965..104	0.742537(18)	0.598306(14)	0.805759(27)
MACHO*05:16:28.5–69:25:36	79..5861.5053	0.747881(18)	0.601368(14)	0.804097(27)
MACHO*05:16:28.5–69:25:36	78..5861..239	0.747873(18)	0.601366(14)	0.804102(27)
MACHO*05:34:31.9–69:45:15	81..8760..204	0.749809(19)	0.603618(16)	0.805029(29)
MACHO*05:15:49.4–68:41:53	2..5750.2010	0.765468(19)	0.617622(15)	0.806856(28)
MACHO*05:09:29.8–68:21:20	2..4788...82	0.768298(19)	0.620344(15)	0.807426(28)
MACHO*05:23:13.8–69:36:36	78..6947.2839	0.783374(20)	0.631034(16)	0.805534(29)
MACHO*05:34:28.5–68:57:01	82..8772...88	0.791231(21)	0.637010(17)	0.805088(31)
MACHO*05:38:45.4–70:36:12	11..9473..117	0.807845(21)	0.650272(17)	0.804947(30)
MACHO*05:21:25.4–69:52:52	78..6701..236	0.809502(21)	0.652649(17)	0.806236(29)
MACHO*05:23:59.1–69:15:31	80..7073..142	0.834865(24)	0.673340(19)	0.806526(33)
MACHO*05:34:34.6–70:18:21	11..8751..129	0.856625(24)	0.689217(19)	0.804573(31)
MACHO*05:46:42.8–70:40:50	12.10803..112	0.859776(24)	0.692219(39)	0.805116(50)

Table 1—Continued

Cepheid <sup>a</sup>	ID <sup>b</sup>	$P_{\text{FO}}$ (days)	$P_{\text{SO}}$ (days)	$P_{\text{SO}}/P_{\text{FO}}$
MACHO*05:24:33.2–70:09:31	7..7181.1511	0.889705(27)	0.715755(21)	0.804485(34)
MACHO*05:21:16.6–69:52:01	78..6580..150	0.896293(39)	0.722064(26)	0.805612(46)
MACHO*05:23:10.0–70:28:45	6..6934...67	0.920143(27)	0.740074(22)	0.804303(34)
MACHO*05:30:11.7–69:52:02	77..8032..175	0.932517(28)	0.751390(28)	0.805765(38)
MACHO*05:49:27.6–71:32:07	15.11153...34	0.963677(36)	0.775241(25)	0.804462(40)
MACHO*05:47:11.7–70:41:11	12.10803...77	1.015125(33)	0.814284(47)	0.802151(53)
MACHO*05:07:44.6–68:35:20	19..4421..403	1.017549(33)	0.816983(27)	0.802893(37)
MACHO*05:21:05.4–68:23:36	3..6602...41	1.081246(40)	0.867335(32)	0.802163(42)
MACHO*05:10:15.3–68:20:28	2..4909...67	1.084094(38)	0.870033(30)	0.802543(40)
MACHO*05:25:59.2–69:49:14	77..7428..149	1.108837(39)	0.895047(58)	0.807194(60)
MACHO*05:45:22.1–70:50:13	12.10558..923	1.119632(40)	0.896647(08)	0.800841(30)
MACHO*05:43:20.9–71:08:49	15.10191...50	1.183158(45)	0.946917(36)	0.800330(43)
MACHO*05:09:08.0–68:56:43	1..4658...66	1.217536(47)	0.978425(38)	0.803611(44)
MACHO*05:07:37.0–69:12:47	1..4412..130	1.217973(48)	0.975255(38)	0.800719(44)
MACHO*05:49:28.9–70:22:40	12.11170...25	1.251635(50)	1.008617(41)	0.805839(46)
MACHO*05:02:09.7–68:51:32	1..3570...55	1.321184(56)	1.059515(45)	0.801944(48)
MACHO*05:20:19.7–70:42:29	13..6446...38	1.341432(57)	1.074945(46)	0.801342(48)
MACHO*05:24:07.4–68:51:15	80..7079...62	1.347889(58)	1.076446(46)	0.798616(49)
MACHO*05:37:36.2–69:44:21	81..9244...71	1.352933(63)	1.081235(50)	0.799179(52)
MACHO*04:54:03.4–68:52:02	18..2239...43	1.364210(59)	1.093286(48)	0.801406(49)

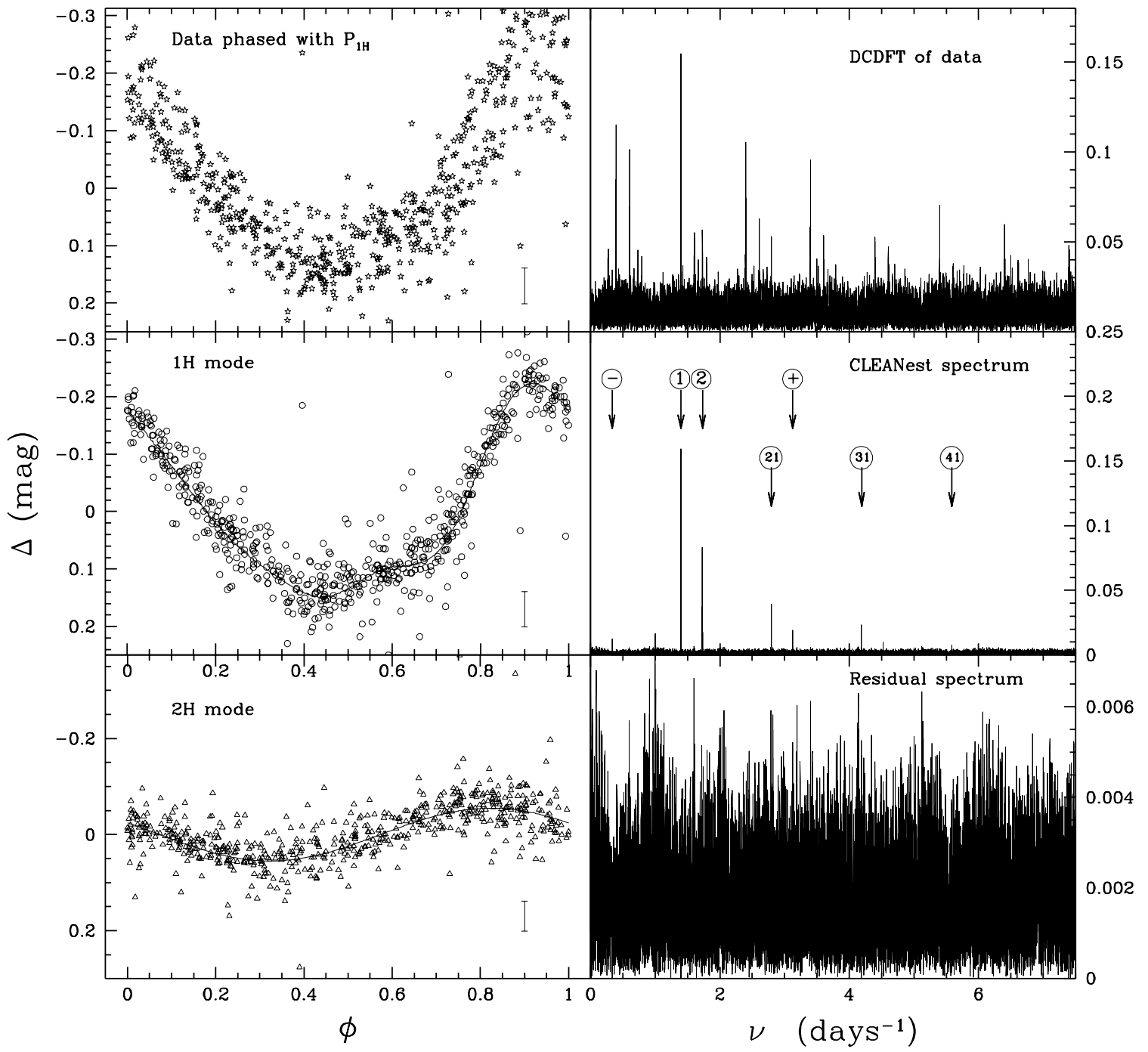
<sup>a</sup>Object designations follow MACHO Project convention: MACHO\*, followed by an object's right ascension and declination (J2000.0).

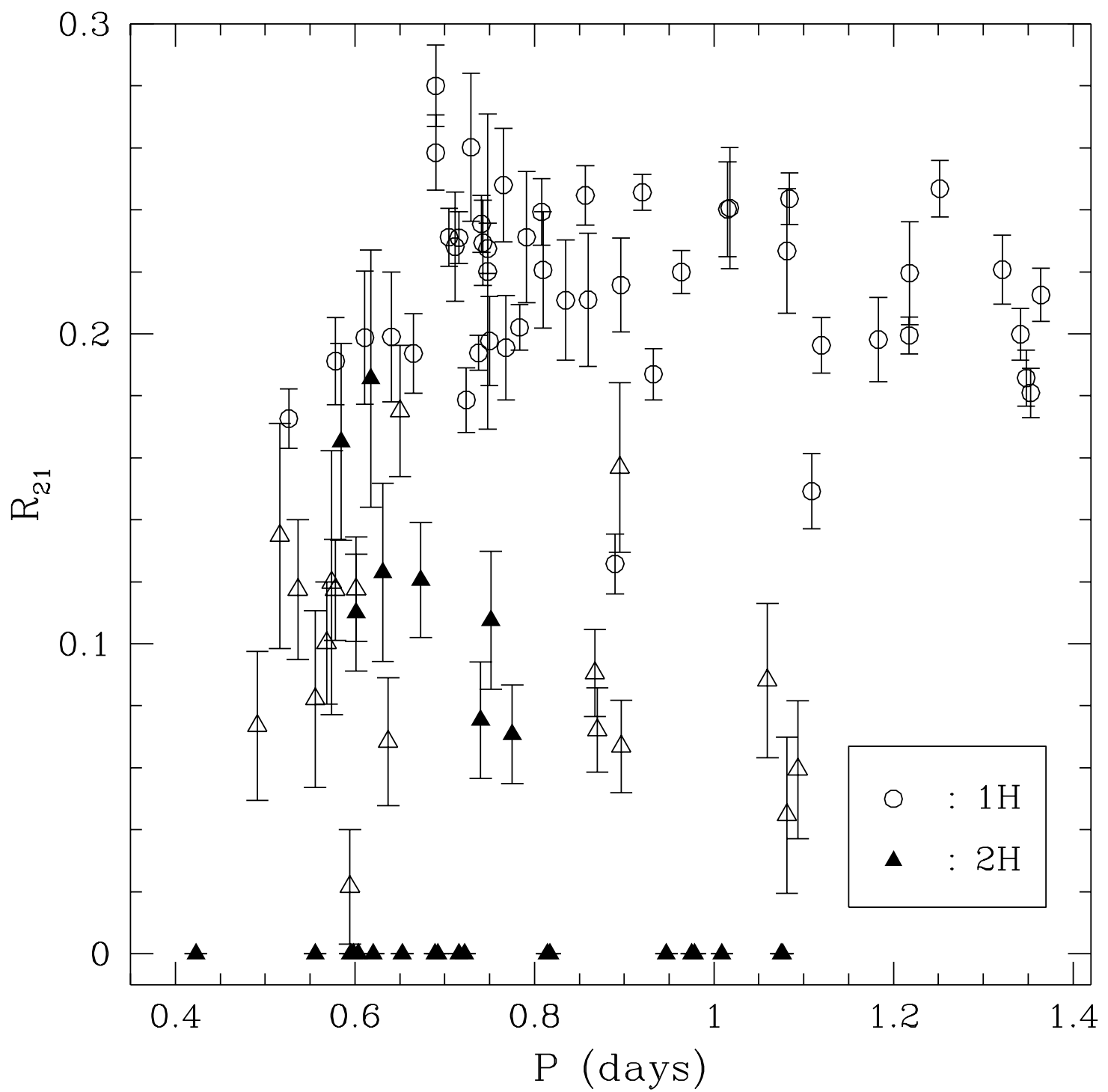
<sup>b</sup>This column contains object designations internal to the MACHO Project.

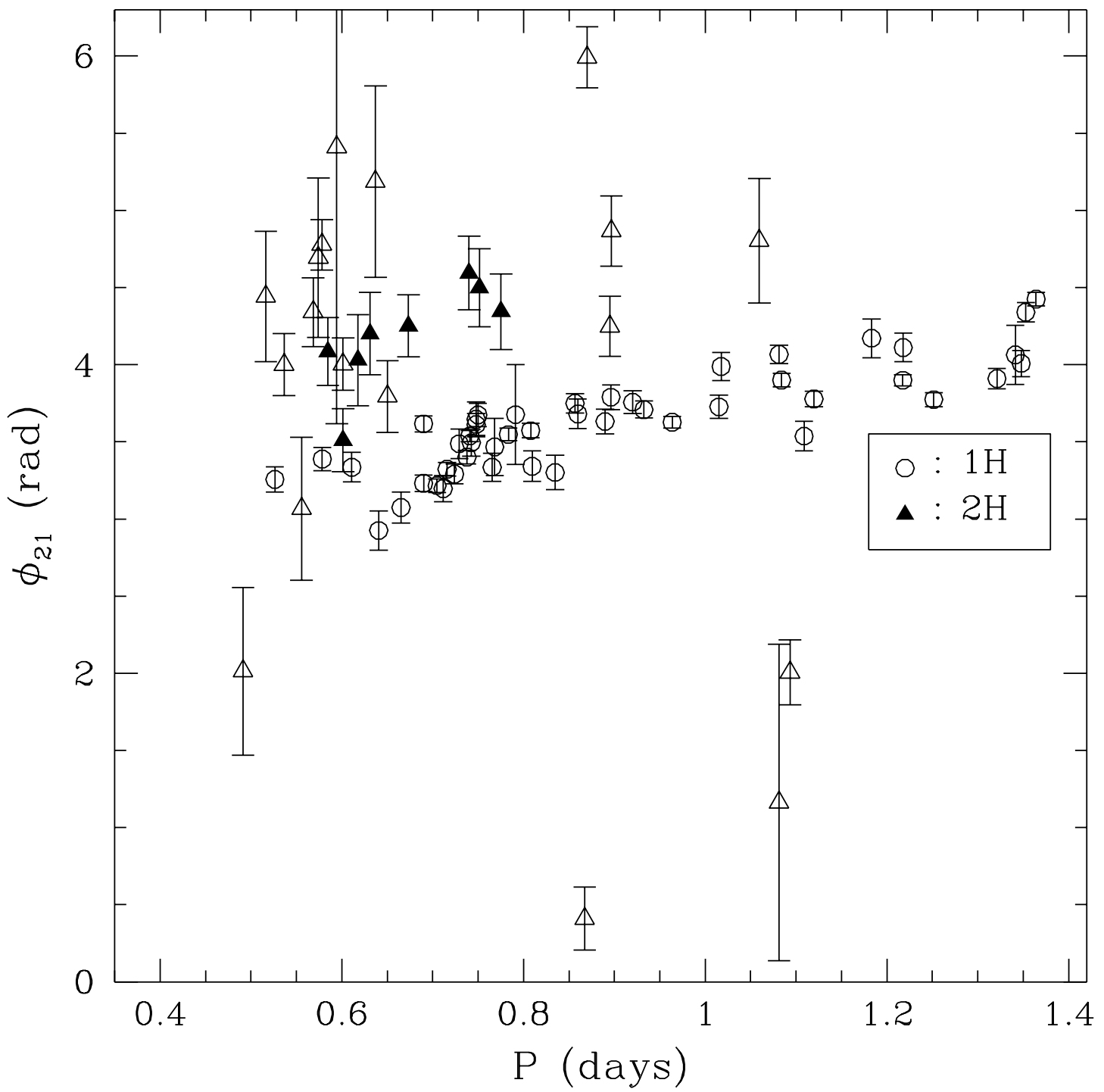
Table 2. Fit Coefficients for MACHO\*05:03:39.6–70:04:32 in Different Bandpasses

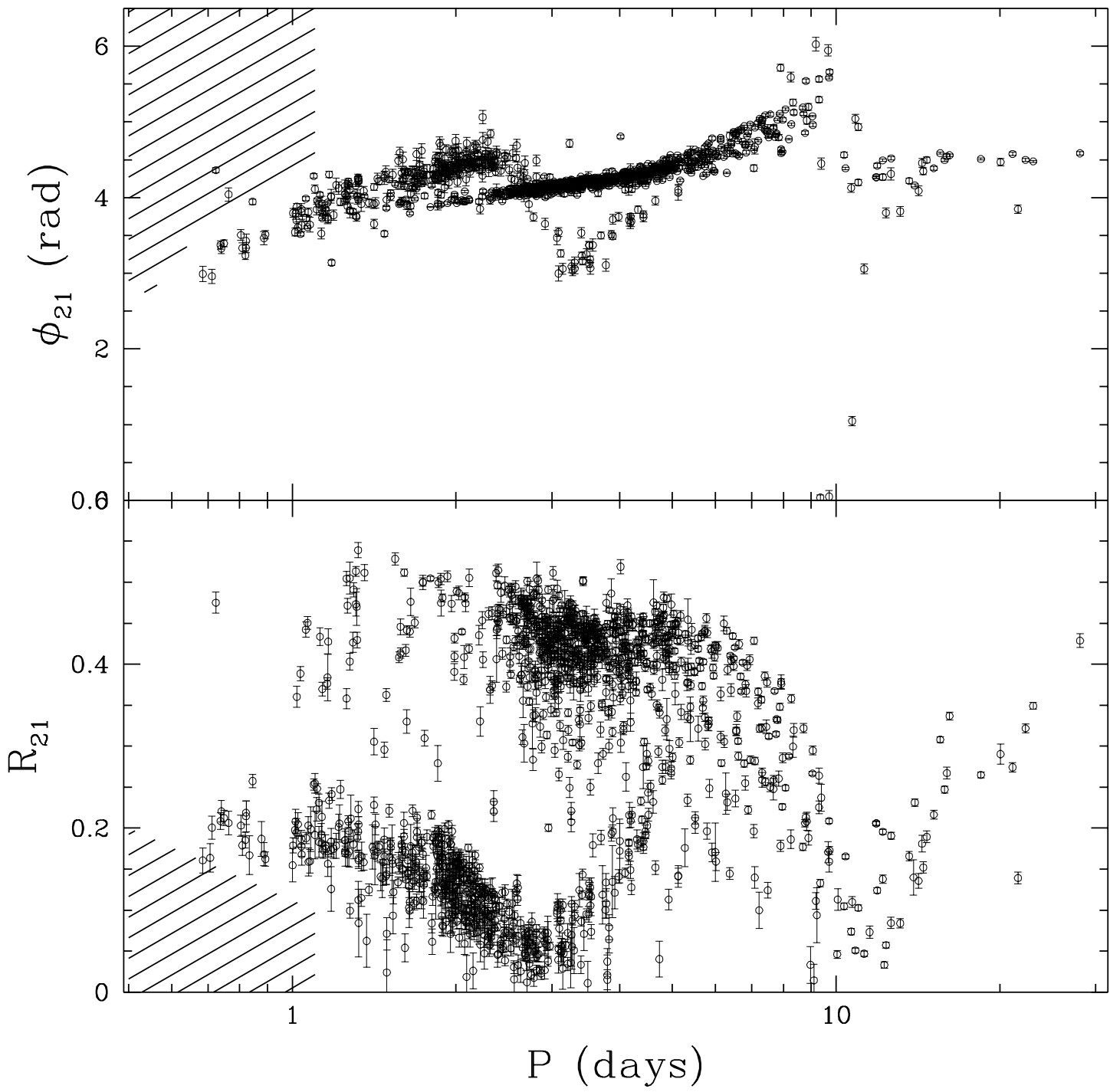
Band, $X$	$X_0$ (mag)	$\Delta_X$ (mag)	$\phi_X$ (rad)	$P_X$ (days)
V	$16.375 \pm 0.030$	$0.0472 \pm 0.0086$	$3.142 \pm 0.034$	$0.775961 \pm 0.000019$
R <sub>KC</sub>	$16.243 \pm 0.030$	$0.0369 \pm 0.0008$	$3.124 \pm 0.043$	$0.775961 \pm 0.000019$

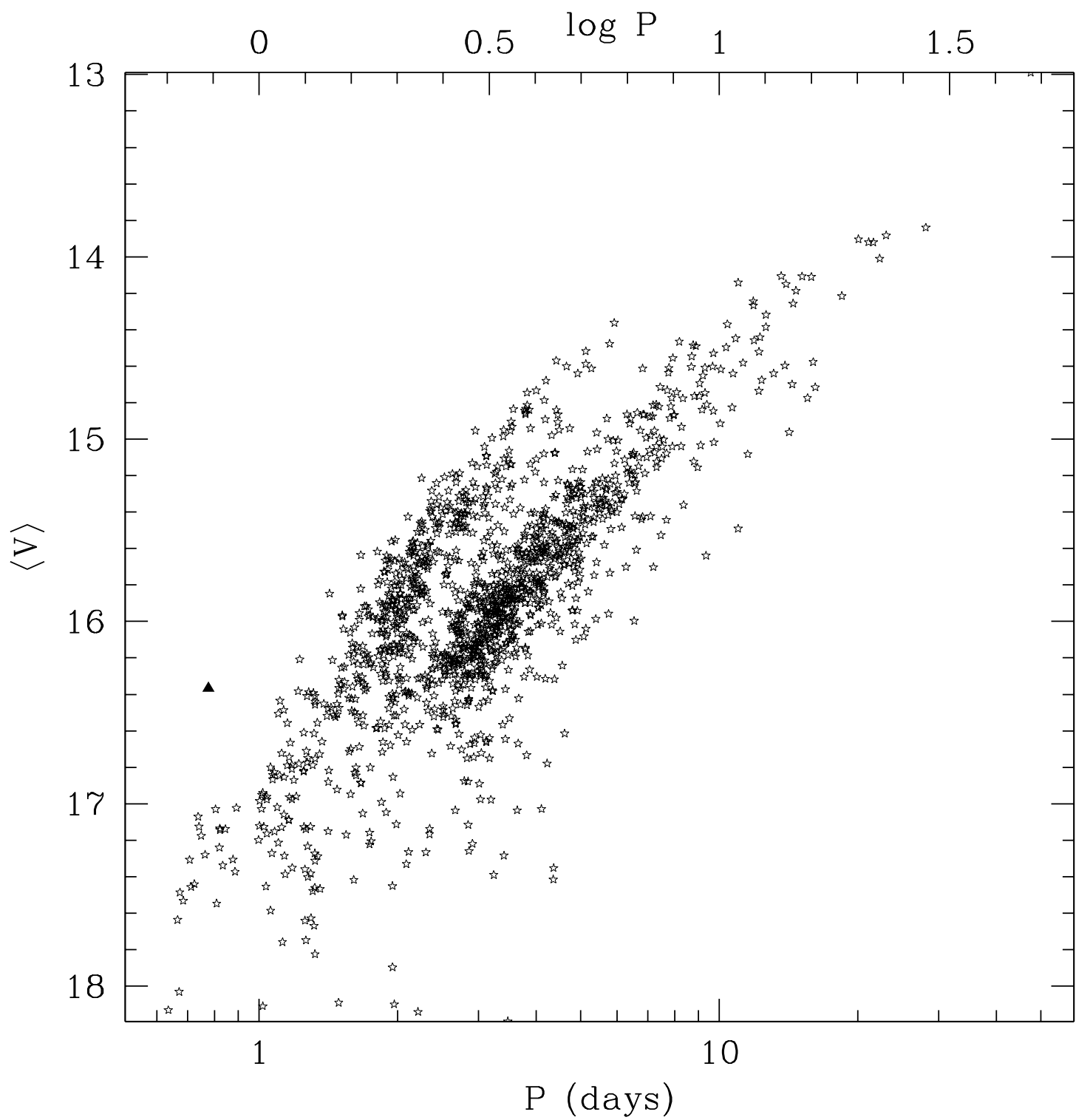
# MACHO\*05:24:13.9–68:49:35

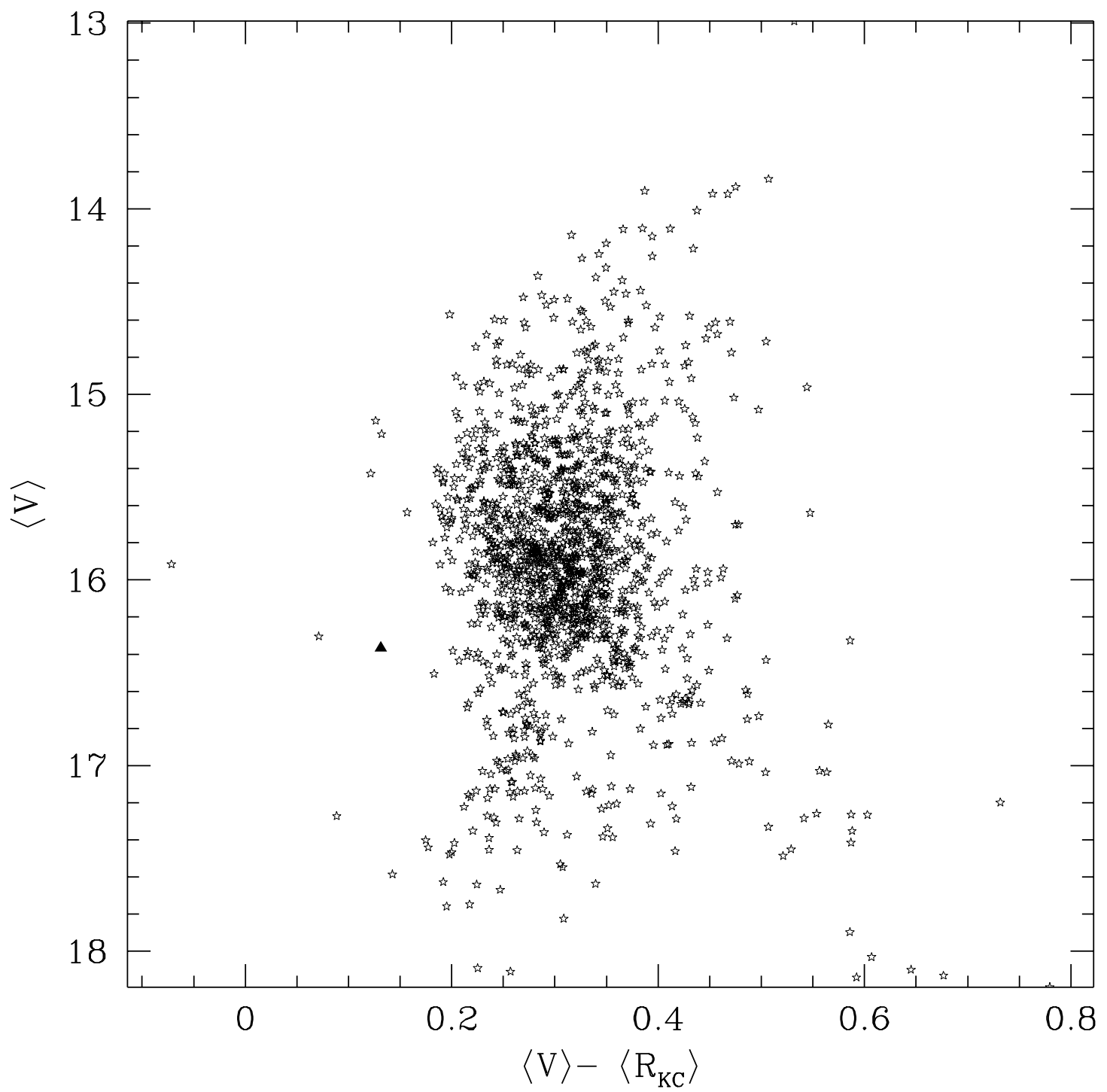












# MACHO\*05:03:39.6-70:04:32

